

Article

# Steep Switching of In<sub>0.18</sub>Al<sub>0.82</sub>N/AlN/GaN MIS-HEMT (Metal Insulator Semiconductor High Electron Mobility Transistors) on Si for Sensor Applications †

Pin-Guang Chen <sup>1,2</sup>, Kuan-Ting Chen <sup>1</sup>, Ming Tang <sup>3</sup>, Zheng-Ying Wang <sup>1</sup>, Yu-Chen Chou <sup>1</sup> and Min-Hung Lee <sup>1,\*</sup> 

<sup>1</sup> Institute of Electro-Optical Science and Technology, National Taiwan Normal University, Taipei 11677, Taiwan

<sup>2</sup> National Nano Device Laboratories, Hsinchu 30078, Taiwan

<sup>3</sup> Device Design Division, PTEK Technology Co., Ltd., Hsinchu 30059, Taiwan

\* Correspondence: mhlee@ntnu.edu.tw; Tel.: +886-2-7734-6747; Fax: +886-2-8663-1954

† This paper is an extended version of our paper published in 7th IEEE International Symposium on Next-Generation Electronics (ISNE 2018), Taipei, Taiwan, 7–9 May 2018.

Received: 6 July 2018; Accepted: 22 August 2018; Published: 24 August 2018



**Abstract:** InAlN/Al/GaN high electron mobility transistors (HEMTs) directly on Si with dynamic threshold voltage for steep subthreshold slope (<60 mV/dec) are demonstrated in this study, and attributed to displacement charge transition effects. The material analysis with High-Resolution X-ray Diffraction (HR-XRD) and the relaxation by reciprocal space mapping (RSM) are performed to confirm indium barrier composition and epitaxy quality. The proposed InAlN barrier HEMTs exhibits high ON/OFF ratio with seven magnitudes and a steep threshold swing (SS) is also obtained with SS = 99 mV/dec for forward sweep and SS = 28 mV/dec for reverse sweep. For GaN-based HEMT directly on Si, this study displays outstanding performance with high ON/OFF ratio and SS < 60 mV/dec behaviors.

**Keywords:** InAlN; swing; wafer-scale; high-electron-mobility transistor (HEMT)

## 1. Introduction

Wide-bandgap GaN-based HEMTs have attracted lots of attention due to sensor applications for gas, pH, and biomedical analyses, etc. [1,2]. How to lower the operation voltage by using steep switching technology is a critical issue in the Internet of Things (IoT) era, which is beneficial for reducing power consumption and improving reliability. Recently, GaN HEMTs based directly on Si have shown advantages and benefits for larger area wafer-scale epitaxy for high throughput mass-production. The incorporation of indium into GaN as a barrier layer improves the power density and reliability because of lattice match for mole fraction ~18% [3,4], as well as higher polarization than possible with the general AlGaIn barrier [5]. The strong spontaneous polarization of InAlN/GaN leads higher 2DEG charge density and drive-current as compared with general AlGaIn/GaN. A lattice-matched InAlN/GaN configuration possessing high chemical and thermal stability is reported with high-temperature 1-MHz large-signal operation at 1000 °C (in vacuum) for 25 h [6]. The InAlN HEMTs thus offer the opportunity of use in environments with temperatures of at least 1000 °C. This characteristic makes high temperature sensor applications feasible. InAlN barrier metal insulator semiconductor high electron mobility transistors (MIS-HEMTs) on sapphire have been demonstrated by the Hong Kong University of Science and Technology (HKUST) [7] with Schottky

source/drain with steep subthreshold swing (SS) behavior and high ON/OFF ratio. The InAlN/GaN on Si with  $\sim 10^7$  and  $10^8$  ON/OFF ratio with Ohmic and hybrid source/drain, respectively, is reported [8,9]. Intel exhibits a near ideal 60 mV/dec of subthreshold swing for MIS-HEMT enhancement mode, and a depletion mode device with steep SS < 60 mV/dec because of “negative” capacitance effect is shown using an AlInN metal-oxide-semiconductor (MOS) HEMT on SiC [10]. The negative capacitance concept is already demonstrated for steep switching on the Complementary Metal-Oxide-Semiconductor (CMOS) platform, including experimental and simulation development [11]. In general, the barrier layer with incorporated In exhibits a steep switch slope, ultra-low drain current leakage floor, and high ON/OFF ratio when compared with AlGaN barriers.

In this study, the  $\text{In}_{0.18}\text{Al}_{0.82}\text{N}/\text{AlN}/\text{GaN}$  directly on Si substrate with dynamic threshold voltage effect for steep switch slope characteristic is demonstrated. The advantages of InAlN HEMTs grown directly on a Si substrate are not only high thermal dissipation, but also high throughput, CMOS-compatible wafer-scale, and low cost, as compared to SiC or sapphire. It should be noted that the thermal conductivity of Si ( $\sim 1.3 \text{ W/cm } ^\circ\text{C}$ ) and SiC ( $\sim 3.6 \text{ W/cm } ^\circ\text{C}$ ) are much higher than sapphire ( $\sim 0.23 \text{ W/cm } ^\circ\text{C}$ ).

## 2. Device Fabrication

The InAlN/AlN/GaN HEMTs structure is grown on the 150 mm/100 mm Si(111) substrate by Metal Organic Chemical Vapor Deposition (MOCVD, Figure 1a), and the schematic diagram of InAlN/AlN/GaN-on-Si MOS-HEMT as shown in Figure 1b. An about 3.9  $\mu\text{m}$ -thick carbon-doped buffer layer and 300 nm i-GaN are deposited. Subsequently, a 2.2 nm AlN spacer is formed to reduce alloy scattering and interface roughness [12]. A strained-layer superlattices (SLS) structure TEM image shown in Figure 2a,c shows several secondary peaks by SLS. Note that the SLS is composed of AlN and GaN supercycles. The purpose is strain relaxation and dislocation pinning at the SLS buffer layer to obtain perfect InAlN/GaN epitaxy. The 6.4 nm barrier layer is grown with  $\text{In}_{0.18}\text{Al}_{0.82}\text{N}$  on the top to form two-dimensional electron gas (2DEGs), as shown in Figure 2b. A capping layer of approximately 2.9 nm  $\text{Al}_2\text{O}_3$  is formed as a gate dielectric and prevents the barrier layer oxidation during the source/drain rapid annealing process. Moreover, the  $\text{Al}_2\text{O}_3$  passivation can improve current collapse at saturation region [13], which is performed for 30 cycles by atomic layer deposition (ALD) using a Fiji-202 DCS (Cambridge NanoTech, Waltham, MA, USA) at 250  $^\circ\text{C}$  with trimethyl-aluminium (TMA) and  $\text{H}_2\text{O}$  as the precursors. For the fabrication process of the devices, the gate-last process is performed. The Ohmic source/drain contacts are placed by the liftoff technique, in which  $\text{Al}_2\text{O}_3$  cap layer is removed in the same layout of lithography step. Ti/Al/Ni/Au (20 nm/120 nm/25 nm/100 nm) is then deposited by Electron-Beam Evaporator with working pressure  $< 4.0 \times 10^{-6}$  Torr. After liftoff processing and cleaning the residual photoresist, rapid thermal annealing (RTA) at 850  $^\circ\text{C}$  for 30 s in high purity  $\text{N}_2$  ambient is performed to form Ohmic contact.

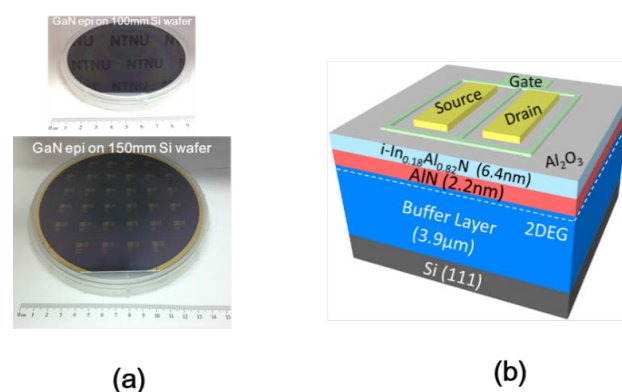


**Figure 1.** (a) GaN-based grown directly on 100 mm and 150 mm Si(111) wafer for CMOS compatible wafer-scale standard. (b) Schematic diagram of InAlN/AlN/GaN-on-Si MOS-HEMT.

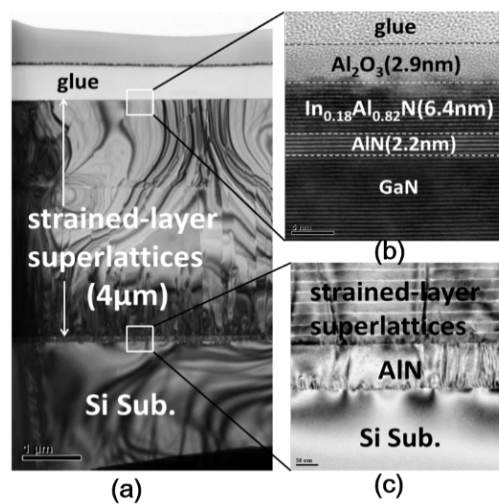


**Figure 2.** (a) GaN-based grown directly on 100 mm and 150 mm Si(111) wafer for CMOS compatible wafer-scale standard. (b) Cross-sectional TEM of 2.9 nm-thick Al<sub>2</sub>O<sub>3</sub> cap layer and In<sub>0.18</sub>Al<sub>0.82</sub>N(6.4 nm)/AlN(2.2 nm) barrier layer. (c) Strained-layer superlattices/AiN on Si substrate.

### 3. Results and Discussion

The sheet resistance and electron mobility of 2DEG obtained in In<sub>0.18</sub>Al<sub>0.82</sub>N/AlN/i-GaN are 527.7 ohm/□ and 820 cm<sup>2</sup>/Vs, respectively, by Hall measurement. The composition of indium = 18% is confirmed from the (002) reflection by HR-XRD as shown Figure 3a, and the same position for InAlN and GaN indicates the lattice-match. Note that the Si peak is the reference and represents InAlN/GaN growing directly on the Si substrate. The multiple peaks indicate a strained-layer superlattice as graded buffer layer. RSM in the (002) and (105) reflection direction indicates strain-free In<sub>0.18</sub>Al<sub>0.82</sub>N/GaN and full relaxation in GaN with a graded buffer layer, respectively, as shown in Figure 3b. The electrical characteristics are performed by a Keithley 4200 semiconductor parameter analyzer—with high power source measure units (SMUs). The transfer characteristics ( $I_{DS}V_{GS}$ ) are shown in Figure 4a with high ON/OFF ratio  $\sim 10^7$  for InAlN device. The off-state current is  $\sim 2 \times 10^{-8}$  A/mm (i.e.,  $2 \times 10^{-11}$  A/μm) with a low leakage current because of the lattice-match between In<sub>0.18</sub>Al<sub>0.82</sub>N and GaN, which is close to the limitation of the measurement instrument and environment ( $\sim 10^{-12}$ – $10^{-15}$  A/μm). Based on Vegard's Law, the lattice is matched and strain free between the In<sub>0.18</sub>Al<sub>0.82</sub>N and GaN heterojunction [14]. The  $I_{GB}$  is  $\sim 10^{-8}$ – $10^{-12}$  A, which is lower than transient current in Figure 4b. Therefore, the gate transient current corresponding to triangular voltage stimulus is contributed by displacement current. The low  $I_{GB}$  is due to Al<sub>2</sub>O<sub>3</sub> as gate dielectric for MOS-HEMT. The saturation drain current ( $I_{Dsat}$ ) of InAlN device is measured  $\sim 125$  mA/mm with  $L_G = 15$  μm at  $V_{DS} = 10$  V and  $V_G = 2$  V. A steep SS that is also obtained in the InAlN device exhibits SS = 99 mV/dec for forward sweep and SS = 28 mV/dec for reverse sweep. For gate bias smaller than  $V_T$ , the channel is not formatted due to no 2DEG. The electrons accumulate on top of GaN to form 2DEG for the channel with gate bias approaching to  $V_T$ , as shown in Figure 5. The fast-current response for transient behaviors between the gate and source/drain shows similarly for InAlN and AlGaN in Figure 4b. The measurement setup is shown in Figure 4c, and the waveform generator/fast measurement unit (WGFMU) module is used. The triangular waveform is applied as blue line in Figure 4b. The voltage range is from  $-7$  V to  $-3$  V to correspond OFF-state to subthreshold region of  $I_{DS}V_{GS}$  in Figure 4a. The gate response current is shown in black and red line in Figure 4b for displacement current, in which it is much higher than DC gate leakage (Figure 4a). Note that the transient current response to the triangular voltage stimulus is used for ferroelectric material polarization by displacement current extraction [15].

With increasing bias, a lower displacement current in InAlN is observed for cases B due to neutralized spontaneous polarization of AlN (Al-rich) and InN (In-rich). For reverse sweep with case C, electrons of acceptor-like traps ( $Q_A$ ) transit to metal electrode as shown in Figure 5 and lead lower displacement current in Figure 4b. This would make the electrons transit from 2DEG to  $Q_A$  at  $\text{Al}_2\text{O}_3/\text{InAlN}$  interface of InN region for reverse sweep to have gate bias approach to  $V_T$ . This results in  $V_T$  being more dynamically positive and SS below 60 mV/dec for reverse sweep in Figure 4a. Finally, the 2DEG is vanished with a gate bias smaller than  $V_T$  and back to the initial state. Note that the higher transient current of AlGaN in case D reflects the higher leakage current in Figure 4b. The asymmetric current with signal up and down (cases A & B vs. C & D in Figure 4b) is because of intrinsic spontaneous polarization in barrier layers. The steep switching in this work is obtained by displacement charge transition effect, which is different with other steep slope transistors technology, such as negative capacitance, threshold selector, TFET (tunneling FET), etc. For negative capacitance, the surface potential or internal gate voltage is amplified by ferroelectric gate stack [16]. The spontaneous rupture of filament is developed in Ag/TiO<sub>2</sub>-based device for threshold selector [17]. For TFET, the steep current increasing is occurred by BTBT (band-to-band tunneling) [18].

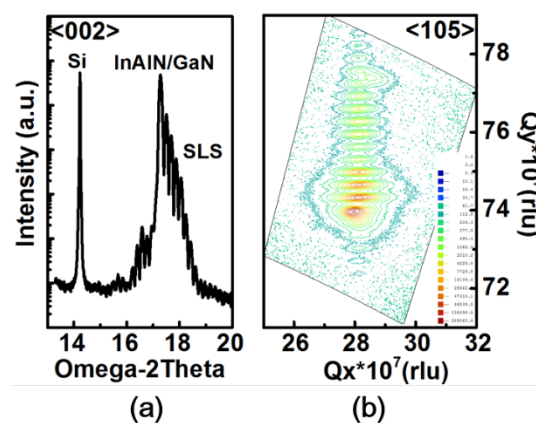


**Figure 3.** (a) High-Resolution X-ray Diffraction (HR-XRD) rocking curve of the (002) peak of InAlN/AlN/GaN-on-Si. The signal peaks of the Si substrate and InAlN or GaN are observed, indicating the Indium-based ternary heterojunction structure grown directly on the Si substrate. (b) RSM (Reciprocal Space Mapping) of InAlN/AlN/GaN on-Si in (002). The peaks are aligned, indicating full relaxation in GaN with a SLS buffer layer and strain free  $\text{In}_{0.18}\text{Al}_{0.82}\text{N}/\text{GaN}$ .

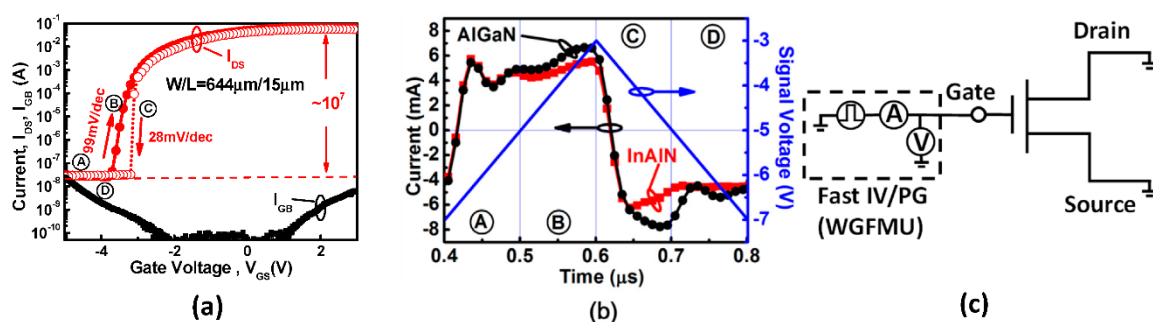


**Figure 4.** (a) The transfer characteristic ( $I_{DS} V_{GS}$ ) of AlGaN/GaN-on-Si and InAlN/AlN/GaN-on-Si MOS-HEMTs. The InAlN device has  $I_{ON}/I_{OFF} \sim 10^7$  and SS = 28 mV/dec covering up to  $\sim 4$  decades in the reverse sweep. The  $I_{GB}$  is lower than  $I_{DS}$ . (b) Transient current of an AlGaN and InAlN device. The asymmetric current with signal up and down is due to intrinsic spontaneous polarization. (c) The measurement setup of transient response by using the waveform generator/fast measurement unit (WGFMU) module.

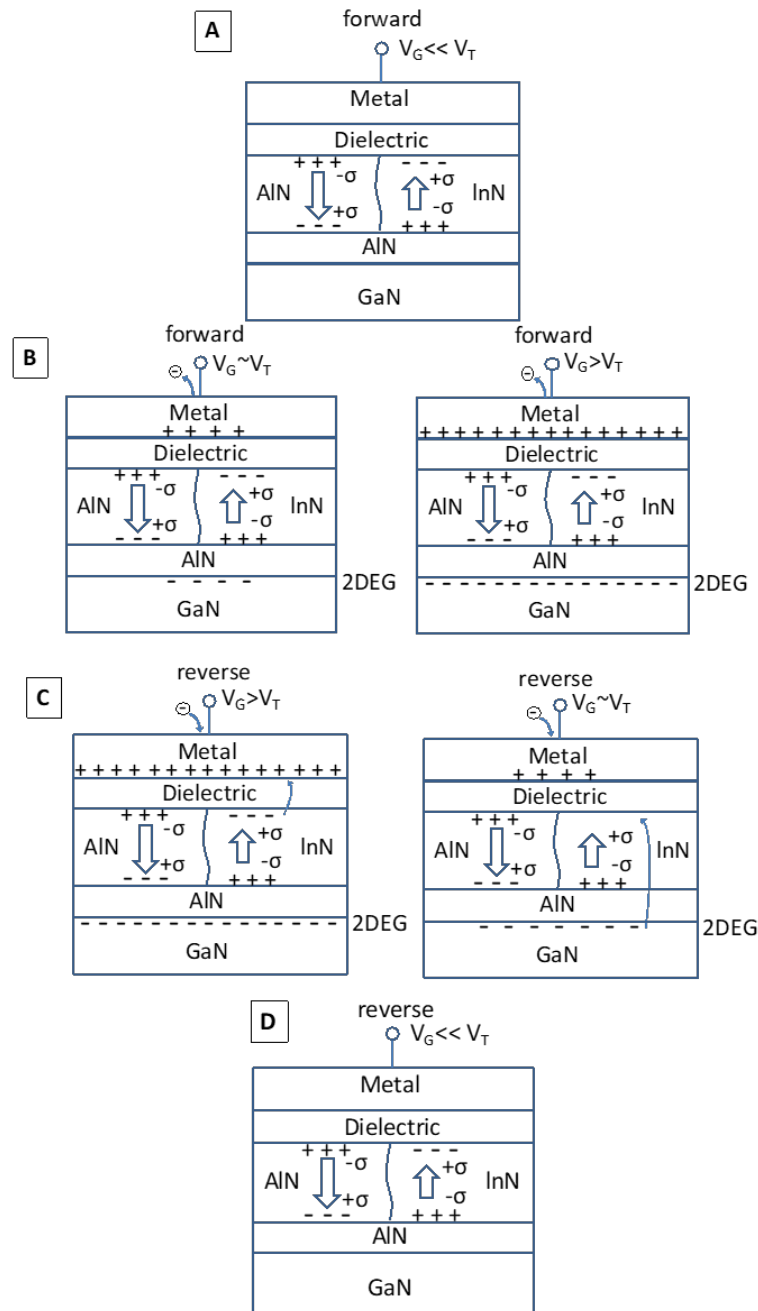


**Figure 5.** Schematic diagram showing the charge balance at case (A–D) in Figure 4. For case C, electrons of acceptor-like traps ( $Q_A$ ) transit to metal electrode and lead to drive out the electrons of 2DEG for reverse sweep. This results in  $V_T$  being more dynamically positive and SS below 60 mV/dec for reverse sweep.

Figure 6 summarizes the GaN-based devices on Si, SiC, and sapphire substrates for ON/OFF ratio and subthreshold swing [7,10,19–23]. This study demonstrates the InAlN barrier GaN MOS-HEMT for SS < 60 mV/dec (reverse sweep SS = 28 mV/dec) with the first time directly-on-Si and outstanding performance with high ON/OFF ratio ( $\sim 10^7$ ). Besides, the ON/OFF ratio of InAlN barrier GaN MOS-HEMT directly-on-Si can be further improved with Schottky-drain contact technology to  $10^8$  [9]. Comparison with different substrate and structure are shown in Figure 6. A steep SS, ultra-low  $I_{OFF}$ , and high ON/OFF ratio of InAlN/GaN on-Si MIS-HEMT are achieved.

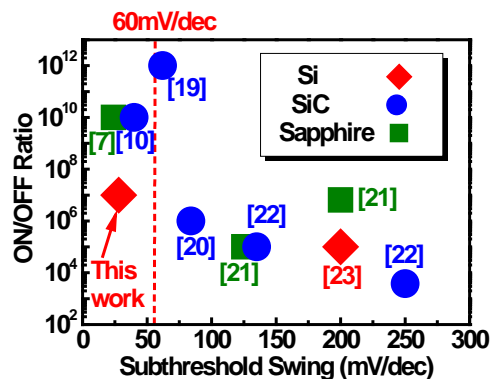


**Figure 6.** ON/OFF ratio vs. subthreshold swing of GaN-based devices on Si, SiC, and Sapphire substrates. This study shows SS < 60 mV/dec of InAlN barrier GaN MOS-HEMT first time directly-on-Si.

#### 4. Conclusions

The heterojunction of  $\text{In}_{0.18}\text{Al}_{0.82}\text{N}$  and GaN with lattice-match is validated by HR-XRD and RSM to confirm the indium barrier composition and epitaxy quality. The proposed promising wafer scale InAlN/Al/GaN HEMT directly-on-Si with steep subthreshold slope (SS < 60 mV/dec) is demonstrated in this study and is attributed to dynamic threshold voltage effect. The performance of the InAlN barrier HEMTs exhibits high ON/OFF ratio with seven magnitudes, and a steep SS is also obtained with SS = 99 mV/dec for forward sweep and SS = 28 mV/dec for reverse sweep. For the on-Si device, this study displays outstanding performance with high ON/OFF ratio and SS < 60 mV/dec behaviors. The steep slope characteristics of InAlN HEMTs growth on a Si substrate is feasible for applications, such as gas, pH, biomedical sensors, etc., and it is beneficial for reducing power consumption and reliability improvement in the IoT era.

**Author Contributions:** P.-G.C. designed the overall architecture of InAlN/AlN/GaN MIS-HEMT and contributed to the implementation and deployment of this work. K.-T.C. was mainly involved in preparing the experimental validation and processing the results. M.T. was a consultant for this work. Z.-Y.W. and Y.-C.C. were focused on the electrical measurement. M.-H.L. has been responsible for proposing the research topic, project administration, funding acquisition, reviewing the work and the paper's preparation.

**Funding:** This research was funded by the Ministry of Science and Technology (MOST 107-2218-E-003-004).

**Acknowledgments:** The authors are grateful for the processing support by the National Nano Device Laboratories (NDL) and Nano Facility Center (NFC), Taiwan.

**Conflicts of Interest:** The authors declare no conflict of interest.

#### References

1. Pearton, S.; Hull, R.; Jagadish, C.; Osgood, R.M.; Parisi, J., Jr.; Wang, Z. *GaN and ZnO-Based Materials and Devices*; Springer Series in Materials Science; Springer: Berlin/Heidelberg, Germany, 2011; Chapter 6; pp. 165–203.
2. Lee, D.-S.; Lee, J.-H.; Lee, Y.-H.; Lee, D.-D. GAN thin films as gas sensor. *Sens. Actuators B* **2003**, *89*, 305–310. [[CrossRef](#)]
3. Lee, H.-S.; Piedra, D.; Sun, M.; Gao, X.; Guo, S.; Palacios, T. 3000-V 4.3-mΩ·cm<sup>2</sup> InAlN/GaN MOSHEMTs With AlGa<sub>N</sub> Back Barrier. *IEEE Electron Device Lett.* **2012**, *33*, 982–984. [[CrossRef](#)]
4. Chung, J.W.; Saadat, O.I.; Tirado, J.M.; Gao, X.; Guo, S.; Palacios, T. Gate-Recessed InAlN/GaN HEMTs on SiC Substrate With Al<sub>2</sub>O<sub>3</sub> Passivation. *IEEE Electron Device Lett.* **2009**, *30*, 904–906. [[CrossRef](#)]
5. Lecourt, F.; Ketteniss, N.; Behmenburg, H.; Defrance, N.; Hoel, V.; Eickelkamp, M.; Vescan, A.; Giesen, C.; Heuken, M.; de Jaeger, J.-C. InAlN/GaN HEMTs on Sapphire Substrate with 2.9-W/mm Output Power Density at 18 GHz. *IEEE Electron Device Lett.* **2011**, *32*, 1537–1539. [[CrossRef](#)]
6. Maier, D.; Alomari, M.; Grandjean, N.; Carlin, J.-F.; Difforte-Poisson, M.A.; Dua, C.; Delage, S.; Kohn, E. InAlN/GaN HEMTs for Operation in the 1000 °C Regime: A First Experiment. *IEEE Electron Device Lett.* **2012**, *33*, 985–987. [[CrossRef](#)]

7. Zhou, Q.; Huang, S.; Chen, H.; Zhou, C.; Feng, Z.; Cai, S.; Chen, K.J. Schottky source/drain Al<sub>2</sub>O<sub>3</sub>/InAlN/GaN MIS-HEMT with steep sub-threshold swing and high ON/OFF current ratio. In Proceedings of the 2011 International Electron Devices Meeting, Washington, DC, USA, 5–7 December 2011.
8. Chen, P.-G.; Tang, M.; Lee, M.H. Indium-Based Ternary Barrier High-Electron-Mobility Transistors on Si Substrate With High ON/OFF Ratio for Power Applications. *IEEE Electron Device Lett.* **2015**, *36*, 259–261. [[CrossRef](#)]
9. Chen, P.-G.; Tang, M.; Liao, M.-H.; Lee, M.H. In<sub>0.18</sub>Al<sub>0.82</sub>N/AlN/GaN MIS-HEMT on Si with Schottky-drain contact. *Solid State Electron.* **2017**, *129*, 206–209. [[CrossRef](#)]
10. Then, H.W.; Dasgupta, S.; Radosavljevic, M.; Chow, L.; Chu-Kung, B.; Dewey, G.; Gardner, S.; Gao, X.; Kavalieros, J.; Mukherjee, N.; et al. Experimental observation and physics of “negative” capacitance and steeper than 40 mV/decade subthreshold swing in Al<sub>0.83</sub>In<sub>0.17</sub>N/AlN/GaN MOS-HEMT on SiC substrate. In Proceedings of the 2013 IEEE International Electron Devices Meeting, Washington, DC, USA, 9–11 December 2013.
11. Ko, E.; Shin, J.; Shin, C. Steep switching devices for low power applications: Negative differential capacitance/resistance field effect transistors. *Nano Converg.* **2018**, *5*, 2. [[CrossRef](#)] [[PubMed](#)]
12. Wu, J.; Walukiewicz, W.; Yu, K.M.; Ager, J.W., III; Li, S.X.; Haller, E.E.; Lu, H.; Schaff, W.J. Universal bandgap bowing in group-III nitride alloys. *Solid State Commun.* **2003**, *127*, 411–414. [[CrossRef](#)]
13. Lee, M.H.; Wei, Y.-T.; Liu, C.; Huang, J.-J.; Tang, M.; Chueh, Y.-L.; Chu, K.-Y.; Chen, M.-J.; Lee, H.-Y.; Chen, Y.-S.; et al. Ferroelectricity of HfZrO<sub>2</sub> in Energy Landscape with Surface Potential Gain for Low-Power Steep-Slope Transistors. *IEEE J. Electron Device Soc.* **2015**, *3*, 377–381.
14. Lee, M.H.; Wei, Y.-T.; Chu, K.Y.; Huang, J.J.; Chen, C.W.; Cheng, C.C.; Chen, M.J.; Lee, H.Y.; Chen, Y.S.; Lee, L.H.; et al. Steep Slope and Near Non-Hysteresis of FETs with Antiferroelectric-Like HfZrO for Low-Power Electronics. *IEEE Electron Device Lett.* **2015**, *36*, 294–296. [[CrossRef](#)]
15. Song, J.; Woo, J.; Prakash, A.; Lee, D.; Hwang, H. Threshold Selector with High Selectivity and Steep Slope for Cross-Point Memory Array. *IEEE Electron Device Lett.* **2015**, *36*, 681–683. [[CrossRef](#)]
16. Lee, M.H.; Lin, J.-C.; Kao, C.-Y. Hetero-Tunnel Field-Effect-Transistors with Epitaxially Grown Germanium on Silicon. *IEEE Trans. Electron Device* **2013**, *60*, 2423–2427. [[CrossRef](#)]
17. Gonschorek, M.; Carlin, J.-F.; Feltin, E.; Py, M.A.; Grandjean, N.; Darakchieva, V.; Monemar, B.; Lorenz, M.; Ramm, G. Two-dimensional electron gas density in Al<sub>1-x</sub>In<sub>x</sub>N/AlN/GaN heterostructures (0.03 ≤ x ≤ 0.23). *J. Appl. Phys.* **2008**, *103*, 093714. [[CrossRef](#)]
18. Lee, D.S.; Laboutin, O.; Cao, Y.; Johnson, W.; Beam, E.; Ketterson, A.; Schuette, M.; Saunier, P.; Palacios, T. Impact of Al<sub>2</sub>O<sub>3</sub> Passivation Thickness in Highly Scaled GaN HEMTs. *IEEE Electron Device Lett.* **2012**, *33*, 976–978. [[CrossRef](#)]
19. Wang, R.; Saunier, P.; Tang, Y.; Fang, T.; Gao, X.; Guo, S.; Snider, G.; Fay, P.; Jena, D.; Xing, H. Enhancement-Mode InAlN/AlN/GaN HEMTs with 10<sup>-12</sup> A/mm Leakage Current and 10<sup>12</sup> ON/OFF Current Ratio. *IEEE Electron Device Lett.* **2011**, *32*, 309–311. [[CrossRef](#)]
20. Wang, R.; Saunier, P.; Xing, X.; Lian, C.; Gao, X.; Guo, S.; Snider, G.; Fay, P.; Jena, D.; Xing, H. Gate-Recessed Enhancement-Mode InAlN/AlN/GaN HEMTs with 1.9-A/mm Drain Current Density and 800-mS/mm Transconductance. *IEEE Electron Device Lett.* **2010**, *31*, 1383–1385. [[CrossRef](#)]
21. Jurkovic, M.; Gregusova, D.; Palankovski, V.; Hascik, S.; Blaho, M.; Cico, K.; Frohlich, K.; Carlin, J.-F.; Grandjean, N.; Kuzmik, J. Schottky-Barrier Normally Off GaN/InAlN/AlN/GaN HEMT With Selectively Etched Access Region. *IEEE Electron Device Lett.* **2013**, *34*, 432–434. [[CrossRef](#)]
22. Lee, D.S.; Chung, J.W.; Wang, H.; Gao, X.; Guo, S.; Fay, P.; Palacios, T. 245-GHz InAlN/GaN HEMTs With Oxygen Plasma Treatment. *IEEE Electron Device Lett.* **2011**, *32*, 755–757. [[CrossRef](#)]
23. Tripathy, S.; Kyaw, L.M.; Dolmanan, S.B.; Ngoo, Y.J.; Liu, Y.; Bera, M.K.; Singh, S.P.; Tan, H.R.; Bhat, T.N.; Chor, E.F. In<sub>x</sub>Al<sub>1-x</sub>N/AlN/GaN High Electron Mobility Transistor Structures on 200 mm Diameter Si(111) Substrates with Au-Free Device Processing. *ECS J. Solid State Sci. Technol.* **2014**, *3*, 84–88. [[CrossRef](#)]

